INTERNATIONAL JOURNAL FOR NUMERICAL METHODS IN FLUIDS, VOL. 8, 305–315 (1988)

TURBULENT FLOW IN A TUBE CONTAINING AN OFFSET ROD

C. W. RAPLEY

Department of Mechanical Engineering, Sunderland Polytechnic, Chester Road, Sunderland, U.K.

SUMMARY

A numerical finite volume prediction method for arbitrary-shaped passages has been applied to the case of fully developed axial turbulent flow past a rod eccentrically placed in a circular tube. The numerical method was based on an orthogonal curvilinear mesh and employed an algebraic stress transport model to calculate the full three-dimensional velocity field directly from the governing partial differential equations. This study is one of a series of applications of this prediction method to a range of different non-circular passages that have been made in order to establish the capabilities and usefulness of this type of procedure. The present eccentric rod case was the subject of a comprehensive experimental investigation by Kacker[1] which has enabled a detailed comparison to be made between the present predictions and the measurements. This comparison included local distributions of axial velocity, wall shear stress and secondary velocities; and although found to be satisfactory overall, some differences in detail revealed possible shortcomings in the measurement of secondary flow. This, together with other previously reported cases, indicates, that, although the present method cannot be expected to replace experiment in providing turbulent passage flow data, it has an important role to play in interpreting and supplementing experiments.

KEY WORDS Turbulent flow Non-circular passage Finite volume

INTRODUCTION

Computer-based numerical methods of solving the governing partial differential equations of recirculating turbulent flow have been available now for well over a decade. The most recent work has tackled the more complex three-dimensional flows where turbulent viscosity based stress models become inadequate. Fully developed turbulent non-circular passage flows are an example of such three-dimensional flows, since the complex stress field gives rise to cross-plane secondary flow circulations which causes a spiralling type flow through the passage. The isotropic turbulent viscosity stress model, be it based on zero-, one- or two-equation turbulence models, cannot be used, since with it stress is directly linked to co-planar strain rates and thus, as with laminar fully developed flow, no cross-plane stresses or flows are predicted and the solution remains just two-dimensional.

The general circulation pattern of the turbulence-driven cross-plane flows has been established from experimental evidence[2–4] as being from the core towards the corners of the duct, recirculating to the core along a path initially parallel to the walls. Typical measured circulation patterns are shown diagrammatically in Figure 1 for three different passages. The secondary velocities were found to be of the order of 1% to 2% of the mean axial velocity, with the maximum velocities being found along the corner bisectors and near the wall. This pattern of cross-plane secondary flow, which can be generalized as from the region of highest axial velocity (core) towards the region of

0271–2091/88/030305–11$05.50 *Received 16 March 1986*

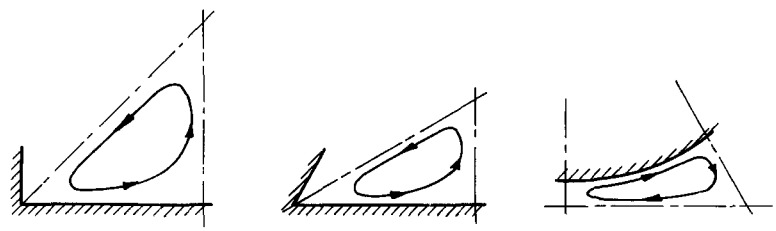

Figure 1. Measured secondary flow circulations

lowest axial velocity (corner regions), is characteristic of turbulence-driven secondary motion in non-circular passages.[5] The convective effects of this motion on local axial velocity distributions are to generally reduce the axial velocity level in the core and increase it in the corner regions. This leads to another characteristic effect, that of increased wall shear in the corner region where it is lowest and decreased wall shear further away from the corner where it is highest to give a more even distribution of wall shear stress than would be expected with no secondary motions. Thus secondary motions act to make the mean flow more evenly distributed.

The early computer-based numerical calculation methods for non-circular passages were simply two-dimensional with secondary flows ignored and stresses calculated with isotropic turbulent viscosity based models.[6,7] However, these methods were found to be little improvement on the earlier graphical methods of such as Deissler and Taylor,[8,9] where errors of up to 100% were found in predictions of local axial velocity or wall shear stress when compared with experiment. It thus became apparent that, although very small when compared with the axial velocity, the convective transport effects of these cross-plane secondary motions on local mean flow were significant and could not be ignored. Some attempts were made, with varying degrees of success, to allow for the effects of secondary flow by methods such as prescribed wall shear stress distributions,[10] prescribed anisotropic turbulent viscosities[11,12] or prescribed elementary secondary flow circulations.[13–15] All of these methods were inevitably limited to particular passage shapes and flow conditions and were dominated by the various prescriptions made.

The pioneer work on numerical computer-based solutions of the full three-dimensional velocity field from the governing partial differential equations was made by Launder and Ying[16] in a study of fully developed square duct flows using a finite volume method based on the turbulent recirculating flow numerical technique of Gosman *et al.*[17] The failure of the isotropic turbulent viscosity based stress model to predict secondary flow meant that a higher-order stress model was needed. This invariably means solution of a partial differential Reynolds stress transport equation for each stress required and results in a complex computer CPU time-consuming multi-equation stress model. However, Launder and Ying were the first to recognize that the stress transport equations could be usefully simplified in the non-circular duct case where, due to the relatively small size of secondary velocities, convective transport effects on the stresses could be neglected as a first approximation. This, together with other simplifications (briefly summarized in Rapley[18]), led to elimination of all terms containing stress gradients and reduced the stress transport equations to a form from which the cross-plane stresses could be extracted as explicit algebraic relations. Axial plane stresses were calculated with an isotropic turbulent viscosity stress model based on a one-equation turbulence model, with turbulence kinetic energy k obtained from solution of its modelled partial differential transport equation and length scales calculated from the geometric formula of Buleev.[19]

The square duct results obtained by Launder and Ying were encouraging in that the secondary

flows generated were of the pattern expected from experiments (see Figure 1) and gave predictions of local mean flow closer to experiment than previous methods which ignored or only approximately accounted for secondary flows.

This success gave rise to a number of further applications of the one-equation method of Launder and Ying, including those for rod bundle passages by Carajilescov and Todreas[20] and Trupp and Aly[21] and for an equilateral triangular duct by Aly *et al.*[3] The predictions were once again found to be encouraging, although in most cases significant simplifications to the method were needed to obtain acceptable results. These simplifications included the neglect of cross-plane shear and prescription of the direction of circulation of the secondary flows generated.

The Launder and Ying algebraic stress transport model was further analysed by Gessner and Emery,[22] who showed that algebraic relations for the axial plane stresses could also be obtained from the simplified stress transport equations. These relations turned out to be similar in form to the isotropic turbulent viscosity relations assumed by Launder and Ying. This gave a set of consistant algebraic relations in which all six (kinematic) components of the stress tensor are explicitly related to the turbulence kinetic energy, k, its dissipation rate ε and gradients of axial velocity (Cartesian co-ordinates with directions 1 and 2 in the cross-plane and 3 in the axial direction):

$$\begin{aligned}
\overline{u_3'^2} &= C_1 k, \\
\overline{u_2'^2} &= C_3 k - C_2 C_4 (k^3/\varepsilon^2)(\partial u_3/\partial x_2)^2 \\
\overline{u_1'^2} &= C_3 k - C_2 C_4 (k^3/\varepsilon^2)(\partial u_3/\partial x_1)^2, \\
\overline{u_1' u_2'} &= -C_2 C_4 (k^3/\varepsilon^2)(\partial u_3/\partial x_1)(\partial u_3/\partial x_2), \\
\overline{u_1' u_3'} &= -C_4 (k^2/\varepsilon)(\partial u_3/\partial x_1), \\
\overline{u_2' u_3'} &= -C_4 (k^2/\varepsilon)(\partial u_3/\partial x_2),
\end{aligned} \tag{1}$$

where C_1, C_2, C_3 and C_4 are related coefficients.

The axial plane (kinematic) shear stresses $\overline{u_1' u_3'}$ and $\overline{u_2' u_3'}$ are seen to be related to co-planar axial strain rates in a turbulent viscosity type model, where

$$\text{turbulent viscosity} \quad \mu_t = C_4 k^2/\varepsilon. \tag{2}$$

In contrast, the cross-plane kinematic stresses $\overline{u_1'^2}$, $\overline{u_2'^2}$ and $\overline{u_1' u_2'}$ are seen to be related to axial strain rates, implying a plausible cause-and-effect connection between these strain rates and cross-plane secondary flow.

This algebraic stress transport model was used by Gosman and Rapley,[23] who reported preliminary results from the present finite volume calculation method which was being developed for fully developed turbulent flow in arbitrary-shaped passages. The method was based on an orthogonal curvilinear mesh which was generated to fit the duct cross-section and employed the $k-\varepsilon$ two-equation turbulence model to calculate the values of k and ε required in the stress model. The potential of this method was demonstrated with the prediction of the triple symmetry of secondary flow obtaining in an equilateral triangular half-duct. Since then the results of further development and applications of the method have been reported[18,24–27] leading to the present application to the case of an offset rod in a circular duct. This case represents a useful two-surface non-circular passage which is a single-rod limiting case of a parallel rod bundle in a casing as well as a particular case of an eccentric annulus. For these and other reasons it was selected as the subject of a detailed experimental study by Kacker[1] and also by the present author as a suitable and interesting case on

which to further test the capabilities and usefulness of the prediction procedure. The present study appears to be the first reported application of a turbulent flow prediction method to this case.

The experiments of Kacker were done with air flow in a circular tube 5·683 inches in diameter, containing an eccentric rod 1·0 inch in diameter located at a radius of 1·113 inches from the tube centre-line. The tube length was 67 equivalent diameters, and axial velocity measurements were made with a double Pitot tube. A boundary layer fence was used for wall shear stress measurements, and secondary velocities were measured with a hot wire anemometer. The velocity probes were introduced into the flow through the tube wall, and most of the measurements presented were for a mean Reynolds number of $2{\cdot}15 \times 10^5$, based on equivalent (hydraulic) diameter. No local turbulence intensity or Reynolds stress measurements were reported.

THE GOVERNING EQUATIONS

The Reynolds equations for steady incompressible turbulent flow were specialized for fully developed flow in straight passages. The Reynolds stresses appearing in these equations were calculated with the algebraic relations given in equations (1). The values of turbulence kinetic energy k and its dissipation rate ε required in these equations were calculated from their partial differential transport equations, in the form normally employed in the widely used k–ε two-equations turbulence model.

All these equations were transformed to general orthogonal co-ordinate form using the method of Pope[28] and then specialized to fully developed flow in straight ducts. Details of the resulting equations can be found elsewhere,[5,18,25] and it is sufficient here to note that the governing transport equations can be written in the following common form:

$$\partial(h_2\rho u_1\phi)/\partial\xi_1 + (h_1\rho u_2\phi)/\partial\xi_2 = \partial(h_2 D_\phi \partial\phi/h_1\partial\xi_1)/\partial\xi_1 + \partial(h_1 D_\phi \partial\phi/h_2\partial\xi_2)/\partial\xi_2 + S_\phi, \quad (3)$$

where ϕ stands for any of the main variables u_1, u_2, u_3, k and ε, D_ϕ is the exchange coefficient and S_ϕ is the source, which is also a receptacle for all the terms not appearing in the remainder of the equation. The full forms of D_ϕ and S_ϕ for each main variable can be found in Table 5.3.1 of Reference 5 or Table 3 of Reference 25. Co-ordinates ξ_1 and ξ_2 are in the cross-plane with metric coefficients h_1 and h_2 and radii of curvature r_1 and r_2 respectively, as illustrated in Figure 2.

The boundary conditions used were entirely conventional, with wall functions employed to cover the region next to the wall. These functions were based on the assumption of one-dimensional flow in turbulence equilibrium, which led to equations based on the well known logarithmic velocity law. The equations obtained for the wall functions for each main variable are given in Reference 25, with full details of their implementation given in Reference 5.

The values of the various constants and coefficients appearing in the governing equations are identical to those used in previous applications of the present method,[18,24,26,27] and no attempt was made to 'tune' them to the present problem.

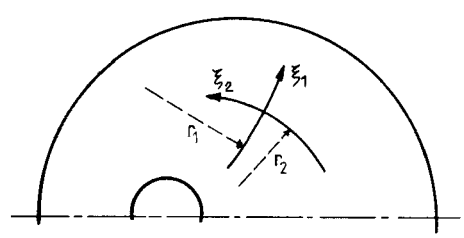

Figure 2. Cross-plane co-ordinate system

THE SOLUTION PROCEDURE

The finite volume solution method used was based on a mesh which was orthogonal curvilinear in the cross-plane as illustrated by the typical portion shown in Figure 3 (full lines), which also shows the cross-plane boundaries of the contiguous control volumes surrounding each main node. These boundary planes, denoted by broken lines, are placed mid-way between the grid lines. A staggered mesh arrangement was used for the cross-plane velocities, as is usually found necessary for stability of recirculating flow calculation procedures.[29] Further details of the mesh arrangement are given elsewhere.[5,25]

The finite volume equivalent of equation (3) was obtained by the micro-integration technique. This led to finite volume equations of the conventional five-point form with coefficients that contained the combined effects of diffusion and convection according to a standard hybrid differencing scheme, which was essentially central differencing with the provision to switch to upwind when convection dominated—see Reference 5 for details.

The cross-plane continuity equation was manipulated into an equation for pressure correction, and the 'SIMPLE' procedure[29] was used for solution of the cross-plane equations. The finite volume equations were solved using an iterative line-by-line ADI solver based on the tridiagonal matrix algorithm.

An orthogonal curvilinear cross-plane mesh was generated in this case from two intersecting families of circular arcs, with one family centred on an axis through the duct and rod centre-plane and the other family centred on an axis normal to this but outside the duct. The grid points of a typical orthogonal mesh generated this way are shown in Figure 3. From symmetry only one half of the duct needed to be considered.

Convergence of the solution was found to be uncertain, due mainly to the coupling and non-linearity of the equations solved. As mentioned earlier, this difficulty was experienced by previous workers, who, with fewer equations to solve, found it necessary to simplify the equations and/or prescribe the circulation direction of secondary flow in order to obtain satisfactory convergence. However, in the present work no simplifications were made, as convergence was obtained through careful linearization of all source terms, the use of block adjustment, under-relaxation and extensive program control. The convergence criterion used was the reduction of the sum of the absolute residuals across the field below a certain prescribed fraction of the axial flux, below which the solution obtained did not significantly change. Typically this fraction was 10^{-3} for axial momentum and 10^{-4} for cross-plane momentum.

Extensive numerical accuracy tests were made on the procedure, concentrating particularly on

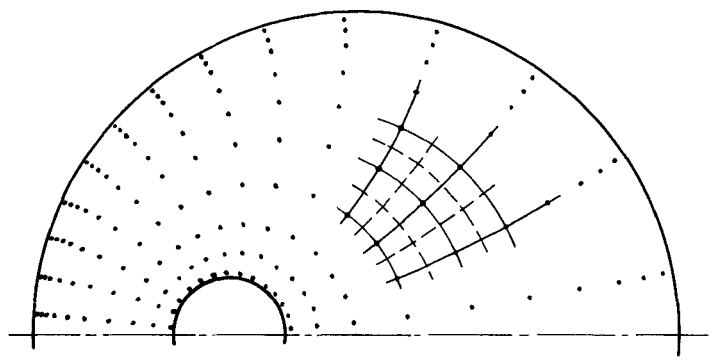

Figure 3. Orthogonal mesh and grid nodes in the cross-plane

the effects of the mesh control volume shape, size and orientation. These tests included comparisons between solutions obtained for particular passage shapes with different meshes, comparison of laminar flow calculations with known analytical solutions, grid refinement and symmetry tests. Examples of the results of these tests are given in References 24, and 25, with full details available in Reference 5.

RESULTS AND COMPARISONS

The predicted secondary flow, in the form of cross-plane secondary velocity vectors, is shown in Figure 4. Two main counter-flowing circulations are evident in the half-duct, which indicates flow from the core towards the gap, along the region around the bisecting plane between the inner and outer surfaces, recirculating to the core via the near surface regions and planes normal to the surfaces through the core. This is entirely consistent with the secondary flow circulations measured and calculated in other non-circular passages, which as mentioned earlier, are from the region of highest axial velocity towards the region of lowest axial velocity, returning via the wall regions.

However, this prediction does not agree with the measurements of Kacker,[1] who obtained only one circulation as seen from his experimental secondary flow streamlines given in Figure 5. It follows that this measured flow pattern also does not agree with the expected flow pattern based on the characteristic pattern of secondary motions expected in non-circular passages from previous measurements. The main difference is the absence in the measurements of a second, counter-

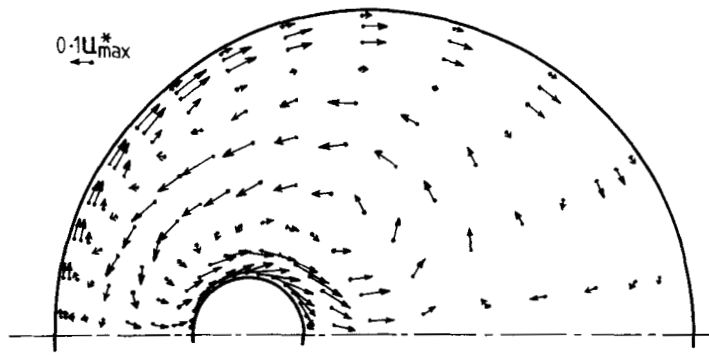

Figure 4. Predicted secondary velocity vectors, $Re = 2{\cdot}15 \times 10^5$

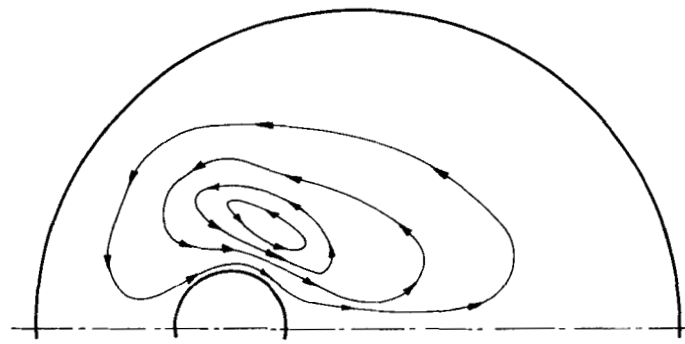

Figure 5. Measured secondary flow streamlines,[1] $Re = 2{\cdot}15 \times 10^5$

rotating circulation in the region next to the outer tube wall. If this missing circulation was present, it would give the expected secondary motion, namely, from the core towards the gap, along the region around the bisecting plane between the two surfaces, dividing in the gap region to recirculate to the core via the two wall regions—as in the present predictions. It could be that this missing circulation was actually there but undetected in the measurements.

A detailed comparison of secondary velocities is given in Figure 6, which shows profiles of the tangential components of secondary velocity (normalized with friction velocity U^*_{3max}) at various angular positions. The calculated profiles compare quite well with the measurements, considering the small size of the velocities, except at the lower values of 'b' (i.e., the 'missing circulation region'), where little or no secondary motion was measured. However, in most cases the measured profiles are such that extrapolations into this region to give possible undetected positive velocities are quite feasible. It may be that the presence of the probe body near the wall (the probe was introduced through the tube wall) in this region made measurements there more uncertain.

Predicted axial velocity contours are compared with the measurements in Figure 7 and show reasonable agreement considering the interpolations involved in both plots. The convective effects of secondary motions are clearly evident, with contours bulging well towards the gap. Figure 8 focuses on the duct centre-plane gap and core axial velocity profiles and shows good agreement between the predictions and the measurements except for a slight overprediction of the core

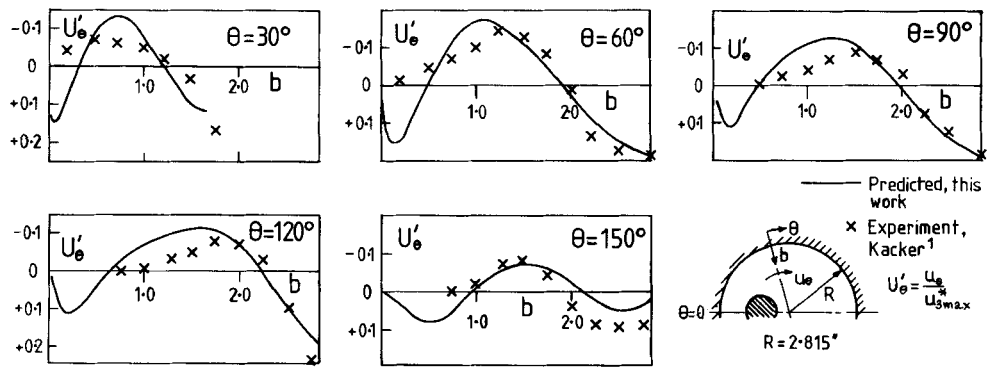

Figure 6. Secondary velocity profiles, $Re = 2{\cdot}15 \times 10^5$

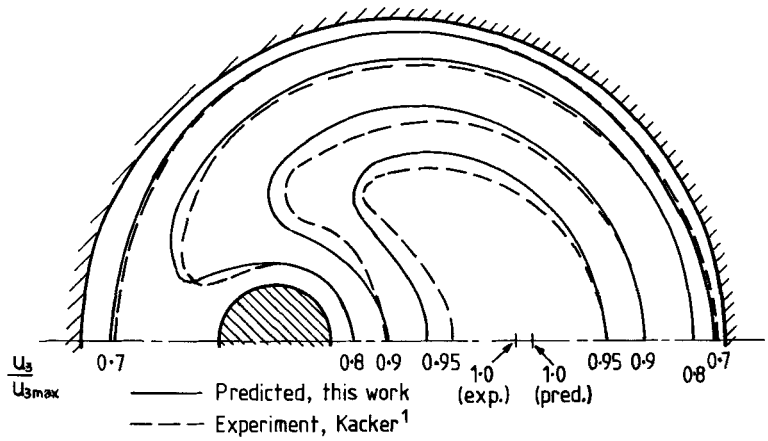

Figure 7. Axial velocity contours, $Re = 2{\cdot}15 \times 10^5$

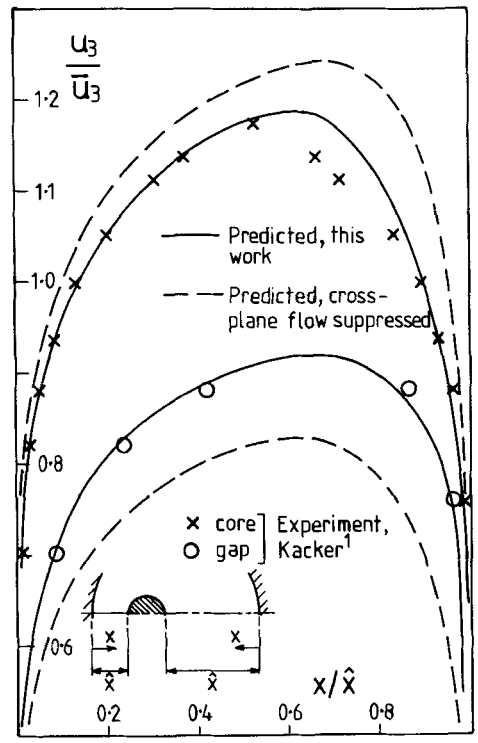

Figure 8. Axial velocity profiles, $Re = 2{\cdot}15 \times 10^5$

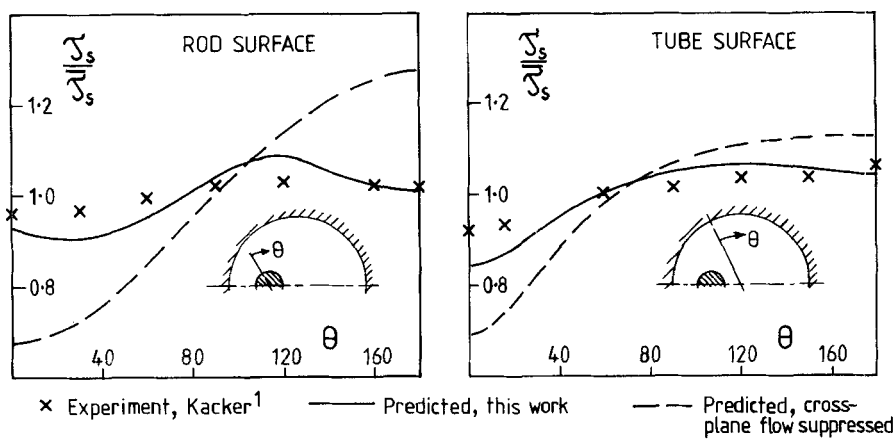

Figure 9. Wall shear stress profiles, $Re = 2{\cdot}15 \times 10^5$

velocity on the rod side of the core. The convective effects of secondary flow are highlighted here by including profiles calculated with secondary motion suppressed. This shows clearly the expected reduced core velocities and increased gap velocities caused by the convective transport effects of secondary flow from the core towards the gap. The good agreement in the gap region implies that the secondary flow convection effect shown in the prediction is valid and provides more evidence that some of this cross-plane convection was there but not recorded in the measurements.

Wall shear stress profiles are plotted in Figure 9 and show the predictions to follow the general

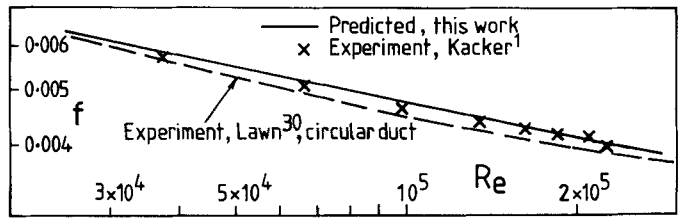

Figure 10. Friction factor characteristics

trends of the measurements but with slightly more variation. The profiles plotted from the calculations made with secondary flow suppressed indicate the considerable reduction in wall shear variation caused by secondary flow, as may be expected from previous studies of such effects in non-circular passages and mentioned earlier in this study. From these previous studies and also in the present study, this reduction in peripheral variation is due to secondary convection towards the wall increasing wall shear stress in regions of low wall shear (gap) and secondary convection away from the wall decreasing wall shear stress in regions of high wall shear (core)—see Figure 4. This secondary motion has occurred in both the measurements and predictions for the rod surface, but is missing from the measurements for the tube surface although it is present in the predictions. However, the relatively high wall shear stress measurements on the tube surface in the gap region contradict this absence and indeed imply even more secondary convection towards the wall there than in the predictions. It appears therefore that the measured wall shear stress profiles provide further evidence of the possible presence of an undetected secondary flow circulation in the tube wall region of the test section.

Figure 10 shows the predicted friction factor characteristic, based on the equivalent (hydraulic) diameter, to be in good agreement with the measurements, particularly at the higher Reynolds numbers. The slight (3%) overprediction at the lower Reynolds numbers is within the 3–4% error band of the measurements quoted by Kacker for the lower Reynolds numbers. The general level of friction factor is seen to be a few per cent higher (e.g., 6% higher at $Re = 10^5$) than the circular duct measurements of Lawn.[30]

CONCLUSIONS

A detailed comparison has been made between predictions of fully developed turbulent flow from a numerical computer-based finite volume procedure calculating the full three-dimensional velocity field and previously published measurements for the case of an offset rod in a circular tube. The calculation method was based on an orthogonal curvilinear mesh and has been developed for general application to arbitrary-shaped ducts, so that no attempt was made to specialize the calculations for this particular case in order to improve agreement between predictions and measurements.

Comparisons between predictions and measurements were made for secondary flows and secondary velocities, axial velocity contours and profiles, wall shear stress profiles and friction factors. Overall agreement between predictions and measurements was found to be satisfactory, although there were disagreements in some important details. The predicted cross-plane secondary motion was consistent with that expected from previous measurements in other non-circular passages, whereas the measurements were not. The indication was of incomplete secondary flow measurement, with a second counter-rotating circulation not detected.

Good agreement between predicted and measured axial velocity profiles, particularly in the gap region where it was demonstrated that the levels were very much dependent on secondary

convection, provided more evidence of possible secondary motions not detected in the measurements. The measured wall shear stress profiles were seen to have slightly less variation than the predictions, which implied significant effects from secondary flow convection which acts, as discussed earlier, to make wall shear stress more uniform. This was particularly so in the gap region, which gave still further support to the view that incomplete secondary velocity measurement could have occurred.

The indication of possible incomplete measurement of secondary flow obtained from the above observations highlights a particular function of the present-day computer-based turbulent flow prediction procedures which the present author believes to be one of the most important and useful—namely that of supplementing and interpreting measurements. Further evidence of the usefulness of the present method in this role has been found in studies of rod bundle passage flows,[25,27] an asymmetrically roughened square duct[5] and flow and heat transfer in a narrow isosceles triangular duct.[26]

In many cases the supplementing role could be used to simplify experiments by eliminating the need to make detailed measurements of local mean and secondary flow; the prediction procedure filling in the detail, using the overall measurements to ensure that the procedure was set up properly. The interpreting role can be used to improve the quality and productivity of the experiments by keeping a check on the consistancy and plausibility of the measurements when they are made. It should be borne in mind of course that the present generation of turbulent flow prediction procedures are far from ideal. However, as methods of stress modelling and calculation of the region close to the wall improve so as to become less dependent on simplifying assumptions, confidence in prediction methods in the above roles can be expected to increase.

REFERENCES

1. S. C. Kacker, 'Some aspects of fully developed turbulent flow in non-circular ducts', *J. Fluid Mech.*, **57,** 583 (1973).
2. E. Brundrett and W. D. Baines, 'The production and diffusion of vorticity in duct flows', *J. Fluid Mech.*, **19,** 375 (1964).
3. A. M. M. Aly, A. C. Trupp and A. D. Gerrard, 'Measurement and prediction of fully developed flow in an equilateral triangular duct', *J. Fluid Mech.*, **85,** 57 (1978).
4. A. Tahir and J. T. Rogers, 'The mechanism of secondary flows in turbulent interchange in rod bundles', *Proc. 7th Canadian Congr. on Applied Mechanics*, 1979, p. 773.
5. C. W. Rapley, 'Fluid and heat flow in tubes of arbitrary cross-section', *Ph.D. Thesis*, University of London, 1980.
6. D. J. Bender, D. M. Switick and J. H. Field, 'Turbulent velocity distribution in a rod bundle', *Report GEAP 5411*, 1967.
7. W. J. Oberjohn, 'Turbulent flow thermal-hydraulic characteristics of hexagonal pitch fuel assemblies', *Liquid-Metal Heat Transfer and Fluid Dynamics*, ASME, 1970, p. 30.
8. R. G. Deissler and M. F. Taylor, 'Analysis of axial turbulent flow and heat transfer through banks of rods or tubes', *Reactor Heat Transfer Conf.*, New York, 1956, Paper No. TID 7529.
9. R. G. Deissler and M. F. Taylor, 'Analysis of turbulent flow and heat transfer in non-circular ducts', *NACA Technical Note 4384*, 1958.
10. M. H. Ibragimov, I. A. Isupov, L. L. Kobzar and V. I. Subbotin, 'Calculation of tangential stresses at the wall of a channel and the velocity distribution in the turbulent flow of a fluid', *Sov. At. Energy*, **21,** 731 (1966).
11. R. Meyder, 'Turbulent velocity and temperature distribution in the central sub-channel of rod bundles', *Nucl. Eng. Design*, **35,** 181 (1975).
12. H. Ramm and K. Johannsen, 'A phenomenological turbulence model and its application to heat transport in inifinite rod arrays with axial turbulent flow', *J. Heat Transfer, Trans. ASME*, **97,** 231 (1975).
13. L. S. Kokorev, A. S. Korsun, B. N. Kostyunin and V. I Petrovichev, 'Hydraulic drag and heat transfer in turbulent flow of liquids in triangular channels', *Heat Transfer Sov. Res*, **3,** 56 (1971).
14. R. Nijsing, 'Heat exchange and heat exchangers with liquid metals', *Report AGARD-LS-57-72*, 1972.
15. R. Gerard, 'Finite element solution for flow in non-circular conduits', *Proc. ASCE*, **100,** 425 (1974).
16. B. E. Launder and W. M. Ying, 'Prediction of flow and heat transfer in ducts of square-section', *Proc. IMechE*, **187,** 455 (1973).
17. A. D. Gosman, W. M. Pun, W. K. Runchal, D. B. Spalding and M. Wolfstein, *Heat and Mass Transfer in Recirculating Flows*, Academic Press, New York, 1969.
18. C. W. Rapley, 'Turbulent flow in a duct with cusped corners', *Int. j. numer. methods fluids*, **5,** 155 (1985).
19. N. I. Buleev, 'Theoretical model of the mechanism of turbulent interchange in fluid flows', *AERE Trans. 957*, 1963.

20. P. Carajilescov and N. E. Todreas, 'Experimental and analytical study of axial turbulent flows in an interior subchannel of a bare rod bundle', *J. Heat Transfer, Trans. ASME,* **98,** 262 (1976).
21. A. C. Trupp and A. M. M. Aly, 'Predicted secondary flows in triangular array rod bundles', *J. Fluids Eng., Trans. ASME,* **101,** 354 (1979).
22. F. B. Gessner and A. F. Emery, 'A Reynolds stress model for turbulent corner flows, Part 1', *J. Fluids Eng., Trans. ASME,* **98,** 261 (1976).
23. A. D. Gosman and C. W. Rapley, 'A prediction method for fully developed flow through non-circular passages', *Proc. Int. Conf. on Numerical Methods in Laminar Turbulent Flow,* Swansea, U. K., 1978, p. 271.
24. A. D. Gosman and C. W. Rapley, 'Fully developed flow in passages of arbitrary cross-section', in C. Taylor and K. Morgan (eds), *Recent Advances in Numerical Methods in Fluids,* Pineridge Press, Swansea, 1980.
25. C. W. Rapley, 'The simulation of turbulent flow and heat transfer in bare rod bundles and other non-circular passages', *Proc. 1982 Computational Fluid Dynamics,* von Karman Institute for Fluid Dynamics, Belgium, 1982.
26. C. W. Rapley and A. D. Gosman, 'The prediction of turbulent flow and heat transfer in a narrow isosceles triangular duct', *Int. J. Heat Mass Transfer,* **27,** 273 (1984).
27. C. W. Rapley and A. D. Gosman, 'The prediction of fully developed axial turbulent flow in rod bundles', *Nucl. Eng. Design,* **97,** 313 (1986).
28. S. B. Pope, 'The calculation of turbulent recirculating flows in general orthogonal co-ordinates', *J. Comput. Phys.,* **26,** 197 (1978).
29. L. S. Caretto, A. D. Gosman, S. V. Patankar and D. B. Spalding, 'Two calculation procedures for steady three dimensional flows with recirculation', *Proc. 3rd Int. Conf. on Numerical Methods in Fluid Mechanics,* Paris, 1972, p. 60.
30. C. J. Lawn, 'The determination of the rate of dissipation in turbulent pipe flow', *J. Fluid Mech.,* **48,** 477 (1971).